subsequent US exposure can induce more efficient cavitation. Inertial cavitation is thought to cause transient disruptions in cell membranes, which enable the transport of extracellular molecules into cells.[11−16] However, US exposure has also induced several biological effects, such as bone fracture healing, wound healing, and induction of apoptosis.[17−19] Moreover, the induced influx of calcium ions, the generation of reactive oxygen species, or the activation of some signals at a cellular level can be attributed to US exposure.[20−23]

Calcium ions (Ca^{2+}) have important roles in cells and are involved in various events such as cell proliferation and cell death.[24,25] US exposure induces the influx of Ca^{2+} by enhancing permeability of the cell membrane. Ca^{2+} also adjusts endosomal acidification and vesicle fusion.[26−29] Therefore, we focused on Ca^{2+} and hypothesized that BLs and US enhance the endosomal escape of gene delivery carriers via Ca^{2+} influx. We also investigated the involvement of ATP in enhanced gene delivery. In this study, we examined the effect of Ca^{2+} and ATP on the endosomal escape and transfection efficiency of AG73-PEG liposomes enhanced by BLs and US exposure.

EXPERIMENTAL SECTION

Materials. The pcDNA3-Luc plasmid, derived from pGL3-basic (Promega, Madison, WI), is an expression vector encoding the firefly luciferase gene under the control of a cytomegalovirus promoter. EGTA (ethylene glycol-bis(2-aminoethyl ether)-*N,N,N′,N′*-tetraacetic acid) was purchased from Sigma (St. Louis, MO). NaF and NaN_3 were purchased from Wako Pure Chemical Industries, Ltd. (Osaka, Japan). Antimycin A was purchased from Enzo Life Sciences, Inc. . (Farmingdale, NY). Alexa Fluor 488-conjugated transferrin was purchased from Molecular Probes, Inc. (Eugene, OR).

Cell Lines and Cultures. A 293T human embryonic kidney carcinoma cell line, stably overexpressing syndecan-2 (293T-Syn2 cell), was cultured in Dulbecco's modified Eagle's medium (DMEM; Kohjin Bio Co. Ltd., Tokyo, Japan), supplemented with 10% fetal bovine serum (FBS; Equitech Bio Inc., Kerrville, TX), penicillin (100 U/mL), streptomycin (100 μg/mL), and puromycin (0.4 μg/mL), at 37 °C in humidified 5% CO_2 atmosphere.

Preparation of AG73-PEG Liposomes. The Cys-AG73 peptide (CGG-RKRLQVQLSIRT) was synthesized manually using the 9-fluorenylmethoxycarbony (Fmoc)-based solid-phase strategy. The peptide was prepared in the COOH-terminal amide form and purified by reverse phase high-performance liquid chromatography. AG73-labeled PEG liposomes were prepared by the hydration method. The pDNA was diluted to a concentration of 0.1 mg/mL in 10 mM HEPES buffer (pH 7.4) and was condensed using 0.1 mg/mL poly-L-lysine (PLL); (SIGMA-Aldrich Co., St. Louis, MO). The complex of pDNA-PLL was added to a lipid film composed of 1,2-dioleoyl-*sn*-glycero-3-phospho-*rac*-1-glycerol (DOPG) (AVANTI Polar Lipids Inc., Alabaster, AL), 1,2-dioleoyl-*sn*-glycero-3-phosphoethanolamine (DOPE) (AVANTI Polar Lipids Inc., Alabaster, AL), and 1,2-distearoyl-*sn*-glycero-3-phosphatidylethanolamine-polyethylene glycol-maleimide ($DSPE-PEG_{2000}$-Mal) (NOF Corporation, Tokyo, Japan) in a molar ratio of 2:9:0.57 followed by incubation for 10 min at room temperature to hydrate the lipids. The solution was sonicated for 5 min in a bath-type sonicator (42 kHz, 100 W) (BRANSONIC 2510J-DTH, Bransoni Ultrasonic Co., Danbury, CT). For coupling, AG73 peptide, at a molar ratio of 5-fold $DSPE-PEG_{2000}$-Mal, was added to the PEG liposomes, and the mixture was incubated for 6 h at room temperature to conjugate the cysteine of Cys-AG73 peptide to the maleimide of the PEG liposomes using a thioether bond. The resulting AG73-peptide-conjugated PEG liposomes (AG73-PEG liposomes) were dialyzed to remove any excess peptide. AG73-PEG liposomes were modified with 5 mol % PEG and 3 mol % peptides.

Preparation of Bubble Liposomes. PEG liposomes composed of 1,2-dipalmitoyl-*sn*-glycero-3-phosphocholine (DPPC) (NOF Corporation, Tokyo, Japan) and 1,2-distearoyl-*sn*-glycero-3-phosphatidylethanolamine-polyethylene glycol ($DSPE-PEG_{2000}$-OMe) (NOF Corporation, Tokyo, Japan) in a molar ratio of 94:6 were prepared by a reverse-phase evaporation method. In brief, all reagents were dissolved in 1:1 (v/v) chloroform/diisopropyl ether. Phosphate buffered saline was added to the lipid solution, and the mixture was sonicated and then evaporated at 47 °C. The organic solvent was completely removed, and the size of the liposomes was adjusted to less than 200 nm using extruding equipment and a sizing filter (pore size: 200 nm) (Nuclepore Track-Etched Membrane, GE Healthcare, U.K.). The lipid concentration was measured using a Phospholipid C test Wako (Wako Pure Chemical Industries, Ltd., Osaka, Japan). BLs were prepared from liposomes using perfluoropropane gas (Takachio Chemical Ind. Co. Ltd., Tokyo, Japan). First, 2 mL sterilized vials containing 0.8 mL of the liposome suspension (lipid concentration: 1 mg/mL) were filled with perfluoropropane gas, capped, and then pressurized with a further 3 mL of perfluoropropane gas. The vials were placed in a bath-type sonicator (42 kHz, 100 W) (BRANSONIC 2510j-DTH, Branson Ultrasonics Co., Danbury, CT) for 5 min to form BLs.

Gene Transfection by AG73-PEG Liposomes with BLs and US Exposure. Two days before the experiments, 293T-Syn2 cells (1×10^5) were seeded in a 48-well plate. The cells were treated with AG73-PEG liposomes (encapsulating pDNA: 3 μg/mL) in serum-free medium for 4 h at 37 °C. The cells were washed twice with Ca^{2+}-free DMEM containing 10 mM EGTA. To deplete ATP, the cells were treated with NaN_3 (0.1%), NaF (10 mM), and antimycin A (1 μg/mL) for 30 min, and then the BLs were added. Within 2 min, US exposure was applied through a 6 mm diameter probe placed in the well (frequency, 2 MHz; duty, 50%; burst rate, 2 Hz; intensity, 1.0 W/cm^2; time, 10 s). A Sonopore 3000 (NEPA GENE, CO., Ltd., Chiba, Japan) was used to generate the US. The cells were transferred to fresh medium and cultured for 20 h, and then luciferase activity was determined.

Measurement of Luciferase Expression. Cell lysates were prepared with lysis buffer (0.1 M Tris-HCl pH 7.8, 0.1% Triton X-100, and 2 mM EDTA). Luciferase activity was measured as relative light units (RLU) per mg of protein using a luciferase assay system (Promega, Madison, WI) and a luminometer (LB96 V, Belthold Japan Co. Ltd., Tokyo, Japan).

Assessment of Localization of pDNA and Transferrin. The 293T-Syn2 cells (7×10^4) were seeded two days before the experiments. The cells were treated with AG73-PEG liposomes (Cy3-labeled pDNA: 3 μg/mL) and Alexa Fluor 488-conjugated transferrin (50 μg/mL) for 4 h at 37 °C. After incubation, the cells were washed, and the BLs (120 μg/mL) were added. Then, US exposure was applied (frequency, 2028 kHz; duty, 50%; burst rate, 2.0 Hz; intensity, 1.0 W/cm^2; time, 10 s). To assess the involvement of Ca^{2+} and ATP, the cells were treated as described in the above section. Subsequently, the cells were incubated for 10 min and then fixed with 4%

paraformaldehyde for 1 h at 4 °C followed by visualization using confocal laser scanning microscopy (CLSM). To differentiate the AG73-PEG liposomes internalized into the cytoplasm following attachment to the surface of the cell membrane, the cytoplasm was distinguished from the cell membrane as shown previously.[9,10,30,31] The rate of colocalization of Cy3-labeled pDNA with Alexa Fluor 488-conjugated transferrin was quantified as follows: amount of colocalization (%) = Cy3 $\text{pixels}_{\text{colocalization}}$/Cy3 $\text{pixels}_{\text{total}} \times 100$, where Cy3 $\text{pixels}_{\text{colocalization}}$ represents the number of Cy3 pixels colocalizing with Alexa Fluor 488-conjugated transferrin and Cy3 $\text{pixels}_{\text{total}}$ represents the total number of Cy3 pixels.

Assessment of Localization of pDNA and lamp-2. The 293T-Syn2 cells were first treated with AG73-PEG liposomes (Cy3-lableled pDNA: 3 μg/mL) for 4 h at 37 °C and then with BLs and US exposure. To assess the involvement of Ca^{2+} and ATP, cells were treated as described in the above section. Subsequently, the cells were incubated for 1 h and then fixed with 4% paraformaldehyde for 1 h at 4 °C. The cells were washed with PBS and permeabilized for 5 min in 0.2% saponin, followed by treatment with 10% goat serum in PBS. Finally, the cells were incubated with anti-lamp2 Ab (Santa Cruz Biotechnology, Inc., Santa Cruz, CA) overnight at 4 °C and treated with Alexa Fluor 488-conjugated secondary Ab (Invitrogen Co., Carlsbad, CA) for 1 h at room temperature in the dark. Then, CLSM and analysis was performed as described in the above section.

■ RESULTS AND DISCUSSION

In previous reports, we have showed that BLs and US exposure could enhance endosomal escape and gene transfection of AG73-PEG liposomes. We have proposed the mechanism that the cavitation induced in the outside of cells by US exposure and BLs could affect endosomes, and then AG73-PEG liposomes internalized by endocytosis escaped from endosomes, leading to enhanced gene expression. It have been also confirmed that AG73-PEG liposomes could not be introduced into cytoplasm directly through the cell membrane after the US-mediated disruption of BLs. However, the exact mechanism of accelerated endosomal escape of carriers was not clear. US exposure induces the influx of Ca^{2+} by enhancing permeability of the cell membrane.[21] In addition, Ca^{2+} adjusts endosomal acidification and vesicle fusion.[26−29] Therefore, to evaluate the mechanism by which BLs and US exposure could promote the endosomal escape of AG73-PEG liposomes, we examined the effect of Ca^{2+} on the endosomal escape and transfection efficiency of AG73-PEG liposomes enhanced by BLs and US exposure. ATP is involved in various reactions, such as acidification of endosomes, intracellular trafficking of vesicles and fusion of vesicles.[26] We also investigated the involvement of ATP-dependent processes in enhanced gene delivery.

First, to evaluate the involvement of Ca^{2+} and ATP in gene expression enhanced by BLs and US exposure, we examined the effect of Ca^{2+} and ATP on gene expression efficiency of AG73-PEG liposomes using 293T-Syn2 cells. The cells were incubated with AG73-PEG liposomes containing pcDNA3-Luc, and then treated with BLs and US exposure. After 20 h incubation, luciferase activity was assayed. BLs and US exposure enhanced the luciferase activity of AG73-PEG liposomes by approximately 60-fold compared to that of AG73-PEG liposomes alone.[9] By contrast, when the cells were treated with 10 mM EGTA before the treatment of BLs and US exposure, the enhancement ratio of luciferase activity by BLs and US exposure was decreased. To examine the effect of ATP on gene transfection efficiency, the cells were treated with NaN_3, NaF, and antimycin A to deplete ATP. The subsequent luciferase assay showed insignificant enhancement by BLs and US exposure. Conversely, when cells were treated with AG73-PEG liposomes alone, luciferase activity was not affected by Ca^{2+} and ATP depletion (Figure 1). These results suggest that

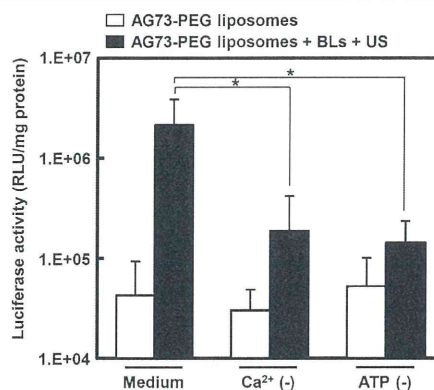

Figure 1. Effects of Ca^{2+} and ATP on gene expression by AG73-PEG liposomes with BLs and US exposure. 293T-Syn2 cells were treated with AG73-PEG liposomes for 4 h at 37 °C, and then cells were washed twice with Ca^{2+}-free DMEM containing 10 mM EGTA for a depleted Ca^{2+} condition. ATP was depleted by pretreating cells for 30 min before US exposure with 1 μg/mL antimycin A, 10 mM NaF, and 0.1% NaN_3. BLs (120 μg/mL) were added to cells followed by immediate US exposure. After replacement with fresh medium, the cells were cultured for 20 h and luciferase activity was determined. The data are shown as the means ± SD ($n = 4$). *$p < 0.05$.

Ca^{2+} and ATP may be necessary to enhance gene transfection efficiency of AG73-PEG liposomes by BLs and US exposure. On the other hand, it is reported that extracellular Ca^{2+} plays important roles to repair the cell membrane disruption and maintain cell survival.[32] Therefore, we examined the cell viability in Ca^{2+}-depleted condition. As a result, in this condition, the cell viability had almost no difference in the treatment with or without BLs and US exposure (data not shown). This result suggested that the decreased enhancement ratio of luciferase activity by the treatment of BLs and US exposure in Ca^{2+}-depleted condition was not due to a change of cell viability.

Recent reports have emphasized the importance of subcellular and intracellular trafficking of gene delivery carriers.[2,3] Among the several steps involeved, endosomal escape is considered one of the most important. In previous study, we have reported that enhanced endosomal escape of AG73-PEG liposomes by BLs and US exposure could increase gene expression.[9] Therefore, we evaluated the involvement of Ca^{2+} and ATP on the endosomal escape of gene delivery carriers. We examined the effects of Ca^{2+} and ATP on localization of pDNA encapsulated in AG73-PEG liposomes and transferrin, as an endosome marker,[33] by confocal microscopy. BLs and US exposure enhanced the endosomal escape of AG73-PEG liposomes and decreased the ratio of colocalization of pDNA and transferrin.[9] The 293T-Syn2 cells were first incubated with AG73-PEG liposomes containing Cy3-labeled pDNA and Alexa Fluor 488-conjugated transferrin and then treated with BLs and US exposure. The cells were observed by confocal microscopy to assess the colocalization of

Cy3-labeled pDNA and Alexa Fluor 488-conjugated transferrin. As shown in Figure 2a, the pDNA internalized into cells were colocalized with transferrin, whereas BLs and US exposure decreased the colocalization of the pDNA and transferrin. However, when cells were treated with 10 mM EGTA, BLs and US exposure did not affect the intracellular localization of the pDNA and transferrin. In the ATP-depleted state, BLs and US exposure had no effect on the intracellular localization of the pDNA and transferrin. Furthermore, we calculated the ratio of colocalization of the pDNA and transferrin and found that BLs and US exposure decreased the ratio of colocalization. By contrast, when cells were treated with 10 mM EGTA or were exposed in an ATP-depleted state, BLs and US exposure did not affect the ratio of colocalization of pDNA and transferrin (Figure 2b). These results suggest that Ca^{2+} and ATP may be required for endosomal escape of AG73-PEG liposomes after the addition of BLs and US exposure.

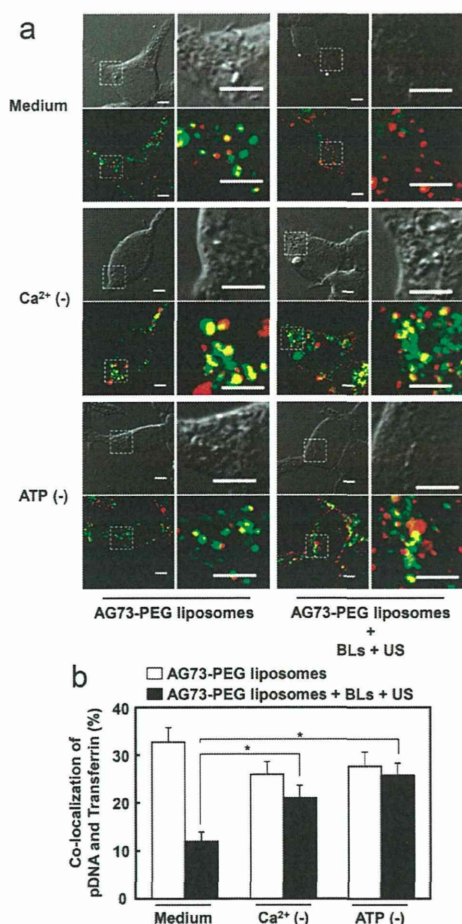

Figure 2. Effects of Ca^{2+} and ATP on intracellular localization of pDNA and endosomes. (a, b) The 293T-Syn2 cells were treated with AG73-PEG liposomes encapsulating Cy3-labeled pDNA (red) and Alexa Fluor 488-conjugated transferrin (green) for 4 h at 37 °C and then washed twice with Ca^{2+}-free DMEM containing 10 mM EGTA to create Ca^{2+}-depleted conditions. ATP was depleted by pretreating cells for 30 min before US exposure with 1 μg/mL antimycin A, 10 mM NaF, and 0.1% NaN_3. BLs (120 μg/mL) were added to cells followed by immediate US exposure. The cells were incubated for 10 min, fixed with 4% paraformaldehyde for 1 h at 4 °C and observed by CLSM. The areas within the dotted square are shown as enlarged images. The scale bars represent 5 μm. The ratio of colocalization of Cy3-labeled pDNA with Alexa Fluor 488-conjugated transferrin was quantified. The data are shown as means ± SE (n = 50). *$p < 0.05$ compared with AG73-PEG liposomes alone (Mann–Whitney's U test).

Efficient gene transfection requires sufficient delivery of genes from the endosomes to the cytosol, to avoid the degradation of genes in lysosomes. Therefore, we assessed the intracellular localization of pDNA and lysosomes and the effects of Ca^{2+} and ATP on localization of pDNA and lysosomes. The 293T-Syn2 cells were treated with AG73-PEG liposomes containing Cy3-labeled pDNA, followed by the addition of BLs and application of US. The cells were fixed and stained with antibodies for lamp-2, a lysosome marker.[34] As a result, the pDNA internalized into cells was colocalized with lamp-2 at 10 or 60 min, whereas BLs and US exposure decreased the colocalization of pDNA and lamp-2 at 60 min after US exposure (Figure3). Moreover, when cells were treated with 10 mM EGTA and depleted of ATP, BLs and US exposure did not decrease the localization of pDNA and lamp-2 (Figure

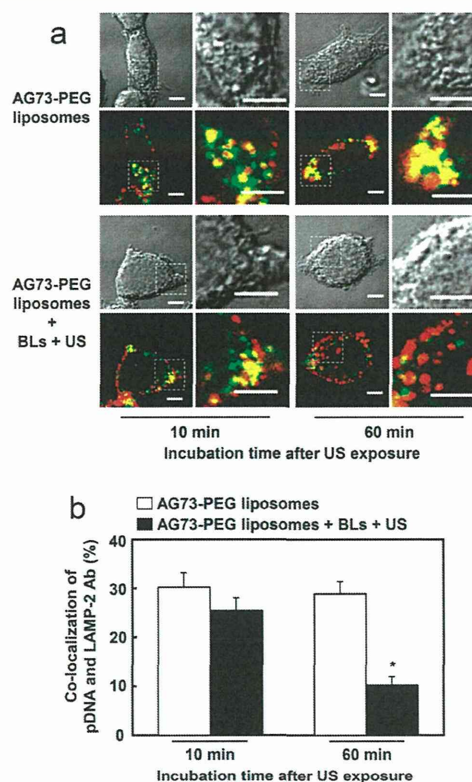

Figure 3. Effect of BLs and US exposure on intracellular localization of pDNA and lysosomes. The 293T-Syn2 cells were treated with AG73-PEG liposomes encapsulating Cy3-labeled pDNA (red) for 4 h at 37 °C. BLs (120 μg/mL) were added to cells followed by immediate US exposure. The cells were incubated for 10 or 60 min and then fixed with 4% paraformaldehyde for 1 h at 4 °C followed by staining with antibodies for lamp-2 (green), a marker for lysosomes. The cells were observed by CLSM. The areas within the dotted square are shown as enlarged images. The scale bars represent 5 μm. The ratio of colocalization of Cy3-labeled pDNA with lamp-2 was quantified. The data are shown as means ± SE (n = 50). *$p < 0.05$ (Mann–Whitney's U test).

4a). We also evaluated the ratio of colocalization of pDNA and lamp-2. In normal medium, the ratio of colocalization of pDNA and lamp-2 was decreased by the application of BLs and US. By contrast, the decrease in the ratio of colocalization of pDNA and lamp-2 could be abrogated by 10 mM EGTA and ATP depletion (Figure 4b). These results suggest that BLs and US exposure could decrease the ratio of colocalization of pDNA and lysosomes. Furthermore, Ca^{2+} and ATP may be involved in the escape of AG73-PEG liposomes from lysosomes. We also confirmed the change of localization of pDNA with endosomes or lysosomes. When 293T-Syn2 cells were treated by AG73-PEG liposomes with BLs and US exposure, a decrease in colocalization of pDNA and endosomes was observed at 10 min after US exposure,[9] whereas a decrease in colocalization of pDNA and lysosomes was observed at 60 min after US exposure (Figure 3). These results suggest that BLs and US exposure might significantly affect endosomes, leading to the decrease in colocalization of pDNA and endosomes. In addition, the increase in the release of genes to the cytosol from endosomes might decrease gene delivery from endosomes to lysosomes.

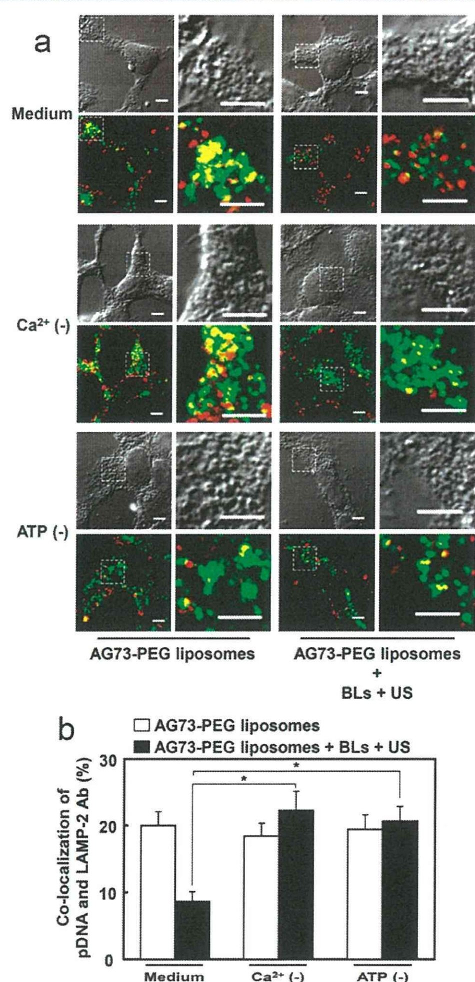

Figure 4. Effects of Ca^{2+} and ATP on intracellular localization of pDNA and lysosome. (a, b) The 293T-Syn2 cells were treated with AG73-PEG liposomes encapsulating Cy3-labeled pDNA (red) for 4 h at 37 °C and then washed twice with Ca^{2+}-free DMEM containing 10 mM EGTA to create Ca^{2+}-depleted conditions. ATP was depleted by pretreating cells for 30 min before US exposure with 1 μg/mL antimycin A, 10 mM NaF, and 0.1% NaN_3. BLs (120 μg/mL) were added to cells followed by immediate US exposure. The cells were incubated for 1 h, fixed with 4% paraformaldehyde for 1 h at 4 °C and stained with antibodies for lamp-2 (green), a marker for lysosomes. The cells were observed by CLSM. The areas within the dotted square are shown as enlarged images. The scale bars represent 5 μm. The ratio of colocalization of Cy3-labeled pDNA with lamp-2 was quantified. The data are shown as means ± SE (n = 50). *$p < 0.05$ (Mann–Whitney's U test).

On the other hand, it has been also reported that US exposure could affect the transcription by oxidative stress or activation of NFκB.[35,36] It may be possible that an activated transcription is involved in enhanced gene transfection. We need more study to clarify the detailed mechanism concerning transcription in the enhanced gene delivery by BLs and US exposure. However, the endosomal escape of AG73-PEG liposomes induced by BLs and US exposure was significantly suppressed in Ca^{2+} or ATP-depleted condition (Figure 3). Therefore, our results suggest that BLs and US exposure can enhance at least the endosomal escape followed by gene expression via Ca^{2+} and ATP.

Although Ca^{2+} and ATP were involved in enhanced endosomal escape and gene expression efficiency of AG73-PEG liposomes by BLs and US exposure, how Ca^{2+} and ATP enhance the endosomal escape of carriers is still unclear. More investigations into the detailed mechanism of enhanced endosomal escape of AG73-PEG liposomes by BLs and US exposure are required. Moreover, endosomal acidification is adjusted by Ca^{2+}, suggesting that the influx of Ca^{2+} by BL and US exposure may affect endosomal acidification.[26] This could lead to the destabilization of endosomes and hydrogen pumps, such as H^+/K^+-ATPase. However, Ca^{2+} and ATP are involved in endosomal membrane fusion.[27,28] Therefore, an influx of Ca^{2+} by BLs and US exposure and ATP may affect endosomal membrane fusion. Our study demonstrated the involvement of Ca^{2+} and ATP in enhanced endosomal escape and gene expression efficiency of AG73-PEG liposomes by BLs and US exposure. Significantly, BLs and US exposure enhanced endosomal escape through biological effects rather than physical effects. In fact, our results suggest that BLs and US exposure could affect more endosomes than lysosomes. It is expected that BLs and US exposure could be safer tools for the enhancement of endosomal escape by setting the appropriate US exposure conditions.

In conclusion, our study focused on Ca^{2+} and ATP and investigated the particular mechanism of enhanced endosomal escape and gene expression of AG73-PEG liposomes by BLs and US exposure. When cells were treated in Ca^{2+}- and ATP-depleted conditions, endosomal escape and gene expression of AG73-PEG liposomes were not enhanced by BLs and US exposure. These results suggest that both Ca^{2+} and ATP are necessary for enhanced endosomal escape and gene expression of AG73-PEG liposomes by BLs and US exposure. These findings may contribute to the development of useful gene transfection methods to achieve efficient gene transfection by improving endosomal escape.

AUTHOR INFORMATION

Corresponding Author

*Tokyo University of Pharmacy and Life Sciences, School of Pharmacy, Drug and Gene Delivery Systems, 1432-1

dx.doi.org/10.1021/mp200606d | *Mol. Pharmaceutics* 2012, 9, 1017–1023

Horinouchi, Hachioji, Tokyo 192-0392, Japan. Tel and fax: +81-42-676-3183. E-mail: negishi@toyaku.ac.jp.

Notes

The authors declare no competing financial interest.

■ ACKNOWLEDGMENTS

We are grateful to Dr. Katsuro Tachibana (Department of Anatomy, School of Medicine, Fukuoka University) for technical advice regarding the induction of cavitation with US, and to Yasuhiko Hayakawa and Kosho Suzuki (NEPAGENE Co., LTD.) for technical advice regarding exposure to US. This study was supported by an Industrial Technology Research Grant (04A05010) from the New Energy and Industrial Technology Development Organization (NEDO) of Japan, a Grant-in-aid for Exploratory Research (18650146) and a Grant-in-aid for Scientific Research (B) (20300179) from the Japan Society for the Promotion of Science, and by a grant for private universities provided by the Promotion and Mutual Aid Corporation for Private Schools of Japan.

■ ABBREVIATIONS USED

BLs, Bubble liposomes; CLSM, confocal laser scanning microscopy; DOPE, 1,2-dioleoyl-*sn*-glycero-3-phosphoethanolamine; DOPG, 1,2-dioleoyl-*sn*-glycero-3-phospho-*rac*-1-glycerol; DSPE, 1,2-distearoyl-*sn*-glycero-3-phosphatidylethanolamine; FBS, fetal bovine serum; Fmoc, fluorenylmethoxycarbonyl; Mal, maleimide; pDNA, plasmid DNA; PEG, polyethylene glycol; US, ultrasound

■ REFERENCES

(1) Zhang, S.; Xu, Y.; Wang, B.; Qiao, W.; Liu, D.; Li, Z. Cationic compounds used in lipoplexes and polyplexes for gene delivery. *J. Controlled Release* **2004**, *100*, 165–180.

(2) Hama, S.; Akita, H.; Ito, R.; Mizuguchi, H.; Hayakawa, T.; Harashima, H. Quantitative comparison of intracellular trafficking and nuclear transcription between adenoviral and lipoplex systems. *Mol. Ther.* **2006**, *13*, 786–794.

(3) Varga, C. M.; Tedford, N. C.; Thomas, M.; Klibanov, A. M.; Griffith, L. G.; Auffenburger, D. A. Quantitative comparison of polyethylenimine formulations and adenoviral vectors in terms of intracellular gene delivery processes. *Gene Ther.* **2005**, *12*, 1023–1032.

(4) Hatakeyama, H.; Ito, E.; Akita, H.; Oishi, M.; Nagasaki, Y.; Futaki, S.; Harashima, H. A pH-sensitive fusogenic peptide facilitates endosomal escape and greatly enhances the gene silencing of siRNA-containing nanoparticles in vitro and in vivo. *J. Controlled Release* **2009**, *139*, 127–132.

(5) Subbarao, N. K.; Parente, R. A.; Szoka, F. C.; Nadasdi, L.; Pongracz, K. pH-dependent bilayer destabilization by an amphipathic peptide. *Biochemistry* **1987**, *26*, 2964–2972.

(6) Lee, S. H.; Choi, S. H.; Kim, S. H.; Park, T. G. Thermally sensitive cationic polymer nanocapsules for specific cytosolic delivery and efficient gene silencing of siRNA: swelling induced physical disruption of endosome by cold shock. *J. Controlled Release* **2008**, *125*, 25–32.

(7) Høgset, A.; Prasmickaite, L.; Selbo, P. K.; Hellum, M.; Engesaeter, B. Ø.; Bonsted, A.; Berg, K. Photochemical internalisation in drug and gene delivery. *Adv. Drug Delivery Rev.* **2004**, *56*, 95–115.

(8) Negishi, Y.; Omata, D.; Iijima, H.; Hamano, N.; Endo-Takahashi, Y.; Nomizu, M.; Aramaki, Y. Preparation and characterization of laminin-derived peptide AG73-coated liposomes as a selective gene delivery tool. *Biol. Pharm. Bull.* **2010**, *33*, 1766–1769.

(9) Negishi, Y.; Omata, D.; Iijima, H.; Takabayashi, Y.; Suzuki, K.; Endo, Y.; Suzuki, R.; Maruyama, K.; Nomizu, M.; Aramaki, Y. Enhanced laminin-derived peptide AG73-mediated liposomal gene transfer by bubble liposomes and ultrasound. *Mol. Pharmaceutics* **2010**, *7*, 217–226.

(10) Omata, D.; Negishi, Y.; Hagiwara, S.; Yamamura, S.; Endo-Takahashi, Y.; Suzuki, R.; Maruyama, K.; Nomizu, M.; Aramaki, Y. Bubble liposomes and ultrasound promoted endosomal escape of TAT-PEG liposomes as gene delivery carriers. *Mol. Pharmaceutics* **2011**, *8* (6), 2416–2423.

(11) Delius, M.; Adams, G. Shock wave permeabilization with ribosome inactivating proteins; a new approach to tumor therapy. *Cancer Res.* **1999**, *59*, 5227–5232.

(12) Taniyam, Y.; Tachibana, K.; Hiraoka, K.; Aoki, M.; Yamamoto, S.; Matsumoto, K.; Nakamura, T.; Ogihara, T.; Kaneda, Y.; Morishita, R. Development of safe and efficient novel nonviral gene transfer using ultrasound: enhancement of transfection efficiency of naked plasmid DNA in skeletal muscle. *Gene Ther.* **2002**, *9*, 260–269.

(13) Negishi, Y.; Matsuo, K.; Endo-Takahashi, Y.; Suzuki, K.; Matsuki, Y.; Takagi, N.; Suzuki, R.; Maruyama, K.; Aramaki, Y. Delivery of an angiogenic gene into ischemic muscle by novel bubble liposomes followed by ultrasound exposure. *Pharm. Res.* **2011**, *28*, 712–719.

(14) Negishi, Y.; Endo, Y.; Fukuyama, T.; Suzuki, R.; Takizawa, T.; Omata, D.; Maruyama, K.; Aramaki, Y. Delivery of siRNA into the cytoplasm by liposomal bubbles and ultrasound. *J. Controlled Release* **2008**, *132*, 124–130.

(15) Negishi, Y.; Endo-Takahashi, Y.; Ishii, K.; Suzuki, R.; Oguri, Y.; Murakami, T.; Maruyama, K.; Aramaki, Y. Development of novel nucleic acid-loaded bubble liposomes using cholesterol-conjugated siRNA. *J. Drug Targeting* **2011**, *19*, 830–836.

(16) Suzuki, R.; Namai, E.; Oda, Y.; Nishiie, N.; Otake, S.; Koshima, R.; Hirata, K.; Taira, Y.; Utoguchi, N.; Negishi, Y.; Nakagawa, S.; Maruyama, K. Cancer gene therapy by IL-12 gene delivery using liposomal bubbles and tumoral ultrasound exposure. *J. Controlled Release* **2010**, *142*, 245–250.

(17) Warden, S. J.; Fuchs, R. K.; Kessler, C. K.; Avin, K. G.; Cardinal, R. E.; Stewart, R. L. Ultrasound produced by a conventional therapeutic ultrasound unit accelerates fracture repair. *Phys. Ther.* **2006**, *86*, 1118–1127.

(18) Warden, S. J. A new direction for ultrasound therapy in sports medicine. *Sports Med.* **2003**, *33*, 95–107.

(19) Feril, L. B. Jr.; Kondo, T.; Zhac, Q. L.; Ogawa, R.; Tachibana, K.; Kudo, N.; Fujimoto, S.; Nakamura, S. Enhancement of ultrasound-induced apoptosis and cell lysis by echo-contrast agents. *Ultrasound Med. Biol.* **2003**, *29*, 331–337.

(20) Juffermans, L. J.; Dijkmans, P. A.; Musters, R. J.; Visser, C. A.; Kamp, O. Transient permeabilization of cell membranes by ultrasound-exposed microbubbles is related to formation of hydrogen peroxide. *Am. J. Physiol.* **2006**, *291*, H1595–H1601.

(21) Juffermans, L. J.; Kamp, O.; Dijkmans, P. A.; Visser, C. A.; Musters, R. J. Low-intensity ultrasound-exposed microbubbles provoke local hyperpolarization of the cell membrane via activation of BK(Ca) channels. *Ultrasound Med. Biol.* **2008**, *34*, 502–508.

(22) Zhou, Y.; Shi, J.; Cui, J.; Deng, C. X. Effects of extracellular calcium on cell membrane resealing in sonoporation. *J. Controlled Release* **2008**, *126*, 34–43.

(23) Takeuchi, R.; Ryo, A.; Komitsu, N.; Mikuni-Takagaki, Y.; Fukui, A.; Takagi, Y.; Shiraishi, T.; Morishita, S.; Yamazaki, Y.; Kumagai, K.; Aoki, I.; Saito, T. Low-intensity pulsed ultrasound activates the phosphatidylinositol 3 kinase/AKT pathway and stimulates the growth of chondrocytes in three-dimensional cultures: a basic science study. *Arthritis Res. Ther.* **2008**, *10*, R77.

(24) Giacomello, M.; Drago, I.; Pizzo, P.; Pozzan, T. Mitochondrial Ca^{2+} as a key regurator of cell life and death. *Cell Death Differ.* **2007**, *14*, 1267–1274.

(25) Hassan, M. A.; Cambell, P.; Kondo, T. The role of Ca^{2+} in ultrasound-elicited bioeffects: progress, perspective and prospects. *Drug Discovery Today* **2010**, *15*, 892–906.

(26) Lelouvier, B.; Puertollano, R. Mucolipin-3 regulates luminal calcium, acidification, and membrane fusion in the endosomal pathway. *J. Biol. Chem.* **2011**, *286*, 9826–9832.

(27) Yan, Q.; Sun, W.; McNew, J. A.; Vida, T. A.; Bean, A. J. Ca^{2+} and N-ethylmaleimide-sensitive factor differentially regulate disassembly of SNARE complexes on early endosomes. *J. Biol. Chem.* **2004**, *279*, 18270–18276.

(28) Mayorga, L. S.; Berón, W.; Sarrouf, M. N.; Colombo, M. I.; Creutz, C.; Stahl, P. D. Calcium-dependent fusion among endosomes. *J. Biol. Chem.* **1994**, *269*, 30927–30934.

(29) Rescher, U.; Zobiack, N.; Gerke, V. Intact Ca2+-binding sites are required for targeting of annxin 1 to endosomal membranes in living HeLa cells. *J. Cell Sci.* **2000**, *113*, 3931–3938.

(30) Suh, J.; Wirtz, D.; Hanes, J. Efficient active transport of gene nanocarriers to the cell nucleus. *Proc. Natl. Acad. Sci. U.S.A.* **2003**, *100*, 3878–3882.

(31) Oba, M.; Aoyagi, K.; Miyata, K.; Matsumoto, Y.; Itaka, K.; Nishiyama, N.; Yamasaki, Y.; Koyama, H.; Kataoka, K. Polyplex micelles with cyclic RGD peptide ligands and disulfide cross-links directing to the enhanced transfection via controlled intracellular trafficking. *Mol. Pharmaceutics* **2008**, *5*, 1080–1092.

(32) Idone, V.; Tam, C.; Goss, J. W.; Toomre, D.; Pypaert, M.; Andrews, N. W. Repair of injured plasma membrane by rapid Ca^{2+}-dependent endocytosis. *J. Cell Biol.* **2008**, *180*, 905–914.

(33) Rothenberger, S.; Iacopetta, B. J.; Kühn, L. C. Endocytosis of the transferrin receptor requires the cytoplasmic domain but not its phosphorylation site. *Cell* **1987**, *49*, 423–431.

(34) Kannan, K.; Stewart, R. M.; Bounds, W.; Carlsson, S. R.; Fukuda, M.; Betzing, K. W.; Holcombe, R. F. Lysosome-associated membrane proteins h-LAMP1 (CD107a) and h-LAMP2 (CD107b) are activation-dependent cell surface glycoproteins in human peripheral blood mononuclear cells which mediate cell adhesion to vascular endothelium. *Cell Immunol.* **1996**, *171*, 10–19.

(35) Kagiya, G.; Ogawa, R.; Ito, S.; Fukuda, S.; Hatashita, M.; Tanaka, Y.; Yamamoto, K.; Kondo, T. Identification of a cis-acting element responsive to ultrasound in the 5′-flanking region of the human heme oxygenase-1 gene. *Ultrasound Med. Biol.* **2009**, *35*, 155–164.

(36) Un, K.; Kawakami, S.; Higuchi, Y.; Suzuki, R.; Maruyama, K.; Yamashita, F.; Hashida, M. Involvement of activated transcriptional process in efficient gene transfection using unmodified and mannose-modified bubble lipoplexes with ultrasound exposure. *J. Controlled Release* **2011**, *156*, 355–363.

NANOMEDICINE

Journal of Controlled Release 160 (2012) 362–366

Contents lists available at SciVerse ScienceDirect

Journal of Controlled Release

journal homepage: www.elsevier.com/locate/jconrel

Prophylactic immunization with Bubble liposomes and ultrasound-treated dendritic cells provided a four-fold decrease in the frequency of melanoma lung metastasis

Yusuke Oda [a,1], Ryo Suzuki [a,1], Shota Otake [a,1], Norihito Nishiie [a], Keiichi Hirata [a], Risa Koshima [a], Tetsuya Nomura [a], Naoki Utoguchi [a], Nobuki Kudo [b], Katsuro Tachibana [c], Kazuo Maruyama [a,*]

[a] *Department of Biopharmaceutics, School of Pharmaceutical Sciences, Teikyo University, Japan*
[b] *Laboratory of Biomedical Engineering, Graduate School of Information Science and Technology, Hokkaido University, Japan*
[c] *Department of Anatomy, School of Medicine, Fukuoka University, Japan*

ARTICLE INFO

Article history:
Received 15 July 2011
Accepted 6 December 2011
Available online 13 December 2011

Keywords:
Dendritic cells
Antigen delivery system
Cancer immunotherapy
Ultrasound
Liposomes

ABSTRACT

Melanoma has an early tendency to metastasize, and the majority of the resulting deaths are caused by metastatic melanoma. It is therefore important to develop effective therapies for metastasis. Dendritic cell (DC)-based cancer immunotherapy has been proposed as an effective therapeutic strategy for metastasis and recurrence due to prime tumor-specific cytotoxic T lymphocytes. In this therapy, it is important that DCs present peptides derived from tumor-associated antigens on MHC class I molecules. Previously, we developed an innovative approach capable of directly delivering exogenous antigens into the cytosol of DCs using perfluoropropane gas-entrapping liposomes (Bubble liposomes, BLs) and ultrasound. In the present study, we investigated the prevention of melanoma lung metastasis via DC-based immunotherapy. Specifically, antigens were extracted from melanoma cells and used to treat DCs by BL and ultrasound. Delivery into the DCs by this route did not require the endocytic pathway. The delivery efficiency was approximately 74.1%. DCs treated with melanoma-derived antigens were assessed for *in vivo* efficacy in a mouse model of lung metastasis. Prophylactic immunization with BL/ultrasound-treated DCs provided a four-fold decrease in the frequency of melanoma lung metastases. These *in vitro* and *in vivo* results demonstrate that the combination of BLs and ultrasound is a promising method for antigen delivery system into DCs.

Crown Copyright © 2011 Published by Elsevier B.V. All rights reserved.

1. Introduction

Melanoma is the most devastating form of skin cancer and represents a leading cause of cancer death. Relative to the tumor mass, melanomas have an early tendency to metastasize; indeed, the majority of melanoma deaths are caused by metastatic disease. As a result, the prognosis for melanoma is poor. In fact, the 5-year survival rate of patients with localized melanoma is up to 90%; in contrast, patients with metastasized melanoma have 5-year survival rates of only 20% [1,2]. Additionally, melanoma is usually resistant to standard chemotherapy, and the response rate for any single agent or combination of agents ranges from 5% to 45% [3,4]. Based on these data, there is a clear need to develop effective therapy for metastasized melanoma. There are various therapeutic methods for metastatic cancer, such as surgical treatment, chemotherapy, radiotherapy, and immunotherapy. Of these methods, immunotherapy may be the most promising because of the possibility of preventing systemic metastasis and recurrence in the long term [5–9].

Dendritic cells (DCs), which are unique antigen-presenting cells capable of priming naive T cells, have been used as vaccine carriers for cancer immunotherapy [6,10]. To induce an effective tumor-specific cytotoxic T-lymphocyte (CTL) response, DCs should abundantly present epitope peptides derived from tumor-associated antigens (TAAs) via major histocompatibility complex (MHC) class I molecules and MHC class II molecules [11]. In general, exogenous antigens (such as TAAs in DCs) are preferentially presented on MHC class II molecules [12,13]. On the other hand, the majority of peptides presented via the MHC class I molecules are generated from endogenously synthesized proteins that are degraded by the proteasome [12]. Therefore, in order to efficiently prime TAA-specific CTLs, it is necessary to develop a novel antigen delivery system that can induce MHC class I-restricted TAA presentation on DCs. Several researchers have studied antigen delivery tools based on the cross-presentation theory of exogenous antigens in DCs [14–19]. Proposed antigen delivery carriers have included liposomes [15,16], poly(γ-glutamic acid) nanoparticles [17], and cholesterol pullulan nanoparticles [18]. All of these carriers deliver the antigens into DCs via the endocytic pathway, inducing the leaking of exogenous antigens from the endosome into the cytosol. Finally, it is thought that the antigens leaked into the cytosol are

Abbreviations: BL, Bubble liposome; CTL, cytotoxic T-lymphocyte; DC, dendritic cell; FITC, fluorescein isothiocyanate; MHC, major histocompatibility complex; MW, molecular weight; PBS, phosphate-buffered saline; TAA, tumor-associated antigen; US, ultrasound.

* Corresponding author at: Department of Biopharmaceutics, School of Pharmaceutical Sciences, Teikyo University, 1091-1 Suwarashi, Midori-ku, Sagamihara, Kanagawa 252-5195, Japan. Tel.: +81 42 685 3722; fax: +81 42 685 3432.
E-mail address: maruyama@pharm.teikyo-u.ac.jp (K. Maruyama).

[1] These authors contributed equally to this work.

0168-3659/$ – see front matter. Crown Copyright © 2011 Published by Elsevier B.V. All rights reserved.
doi:10.1016/j.jconrel.2011.12.003

presented on MHC class I molecules. As an alternative, we have sought to use an antigen delivery system that does not rely on the endocytic pathway.

Multiple papers have reported the use of microbubbles for ultrasound-mediated gene and drug delivery [20–26]. In this delivery system, microstreams and microjets, which are induced by disruption of nano/microbubbles exposed to ultrasound, promote the transfer of extracellular materials into cells by opening transient pores in the cell membrane [27,28]. Previously, we described ultrasound-mediated antigen delivery in DCs using Bubble liposomes (BLs) containing perfluoropropane, an ultrasound imaging gas [29]. Using this system, a model antigen (ovalbumin) could be delivered into the cytosol of DCs independent of the endocytic pathway. This technique provided direct entry of the exogenous antigens into the MHC class I presentation pathway, resulting in the priming of exogenous antigen-specific CTLs. We proposed that this system could facilitate the delivery of crude antigens (such as tumor lysates and extracts) because such substrates could enter cells via a transient pore. In the present study, we used fluorescein isothiocyanate (FITC)-dextran as a substrate to characterize antigen delivery by BLs and ultrasound. Additionally, we assessed the possible application of BLs and ultrasound in DC-based immunotherapy in an *in vivo* model of melanoma. Specifically, we delivered tumor-extracted antigens into DCs using BLs and ultrasound, and investigated whether these treated DCs protected mice from lung metastasis.

2. Materials and methods

2.1. Cells

B16/BL6 cells, a C57BL/6-derived melanoma cell line, were cultured in RPMI 1640 (Sigma Co., St. Louis, MO, USA) supplemented with 10% heat inactivated fetal bovine serum (FBS, GIBCO, Invitrogen Co., Carlsbad, CA, USA), 50 U/ml penicillin, and 50 μg/ml streptomycin (Wako Pure Chemical Industries, Osaka, Japan).

2.2. Generation of mouse bone marrow-derived DCs

DCs were generated from bone marrow cells, as described elsewhere [30]. Briefly, bone marrow cells were isolated from C57BL/6 mice and were cultured in RPMI 1640 supplemented with 10% FBS, 50 μM 2-mercaptoethanol (Sigma Co., St. Louis, MO, USA), 50 U/ml penicillin, 50 μg/ml streptomycin, and 40 ng/ml mouse granulocyte-macrophage colony-stimulating factor (GM-CSF, PeproTech Inc., Rocky Hill, NJ, USA). After 8–16 days of culture, non-adherent cells were collected and used as DCs.

2.3. Preparation of BLs

Liposomes composed of 1,2-distearoyl-sn-glycero-phosphatidylcholine (DSPC) (NOF Co., Tokyo, Japan) and 1,2-distearoyl-sn-glycero-3-phosphatidyl-ethanolamine-methoxypolyethyleneglycol (DSPE-PEG (2 k)-OMe (NOF Co.)), 94:6 (mol:mol), were prepared by reverse phase evaporation. BLs were prepared from the liposomes and perfluoropropane (Takachiho Chemical Industrial Co., Ltd., Tokyo, Japan) as reported before [31,32]. Briefly, 5-ml sterilized vials containing 2 ml of the liposome suspension (lipid concentration: 2 mg/ml) were filled with perfluoropropane, capped, and then supercharged with 7.5 ml of perfluoropropane. The vials were placed in a bath-type sonicator (42 kHz, 100 W; BRANSONIC 2510J-DTH, Branson Ultrasonics Co., Danbury, CT, USA) for 5 min to form the BLs. In this method, the liposomes were reconstituted by sonication under the condition of supercharge with perfluoropropane in the 5-ml vial container. At the same time, perfluoropropane would be entrapped within lipids as micelles (composed of DSPC and DSPE-PEG(2k)-OMe), so forming nanobubbles. The lipid nanobubbles were encapsulated within the reconstituted liposomes, the sizes of which were increased from ~150–200 nm to ~500 nm.

2.4. Extraction of antigens from B16/BL6 cells

The extraction of antigens from B16BL/6 cells was performed by a butanol extraction method [33]. B16/BL6 cells were washed twice with phosphate-buffered saline (PBS) and then incubated with PBS containing 2.5% (v/v) 1-butanol. The solution was collected and centrifuged twice at 1600 ×g at 4 °C. The supernatant was dialyzed with water using a Spectra/Por Dialysis Membrane (MWCO: 10,000; Spectrum Laboratories, Inc., Rancho Dominguez, CA, USA). The dialysate then was centrifuged at 1600 ×g at 4 °C, and the resulting supernatant was freeze-dried.

2.5. FITC-dextran or B16/BL6-extracted antigen delivery following inhibition of the endocytic pathway in DCs

B16/BL6-extracted antigens were labeled with Alexa Fluor 633 Succinimidyl Esters (Invitrogen Co., Carlsbad, CA, USA) (Alexa-B16/BL6). DCs were pretreated with OptiMEM (Invitrogen Co.) containing 10 mM NaN_3 for 1 h at 4 °C to inhibit the endocytic pathway [34,35]. After washing the cells, BLs (120 μg) and FITC-dextran (Sigma Co.) or Alexa-B16/BL6 were added to the DCs in OptiMEM containing 10 mM NaN_3. The DCs were exposed to ultrasound (frequency: 2 MHz, duty: 10%, burst rate: 2.0 Hz, intensity 2.0 W/cm^2, time: 3 × 10 s (interval: 10 s)) using a Sonopore 4000 (6-mm diameter probe; Nepa Gene Co. Ltd., Chiba, Japan), then washed with PBS containing 10 mM NaN_3. The delivery efficiency of FITC-dextran or Alexa-B16/BL6 delivery was analyzed by flow cytometry [36].

2.6. Immunization with antigen-loaded DCs following BLs and ultrasound

DCs (2.5 × 10^5 cells) were pulsed with antigens (50 μg) exposed to ultrasound and/or BLs (120 μg) in a 48-well plate; the contents of 10 wells then were collected, pooled, and seeded into 1 well of a 6-well plate. After 1 h of incubation at 37 °C, the DCs were washed with medium and cultured for 24 h at 37 °C. The cells were washed with PBS, and the DCs (1 × 10^6 cells/100 μl) then were injected intradermally into the backs of C57BL/6 mice twice with a one-week interval.

2.7. B16/BL6 experimental lung metastasis model

C57BL/6 mice were immunized twice with DCs as described above. Seven days after the second immunization, B16/BL6 cells (1 × 10^5 cells/100 μl) were injected into the tail vein. The mice were sacrificed two weeks after the tumor cell injection, and the lungs were harvested and fixed in neutral buffered formalin (10%). The number of B16/BL6 colonies present on the surface of each set of lungs was determined by visual inspection using a stereoscopic dissecting microscope [37].

2.8. Statistical analysis

Differences in the number of lung metastatic colonies between the experimental groups were compared using non-repeated measures analysis of variance (ANOVA) with post-hoc Dunnett's test.

3. Results

3.1. FITC-dextran delivery into DCs by BLs and ultrasound

In BL/ultrasound antigen delivery, extracellular antigens are delivered into cells via the formation of transient membrane pores. Therefore, this technique is expected to deliver antigens into DCs as a function of both

pore size and molecular substrate size. In the present study, we used various molecular weight (MW) FITC-dextran molecules as model antigens and assessed the delivery efficiency of FITC-dextran into DCs. (Fig. 1(a–c)). In DCs treated with FITC-dextran (MW 4000) alone, the mean fluorescence intensity was 4-fold higher than non-treated DCs (Fig. 1(a)). On the other hand, upon treatment with FITC-dextran, BLs, and ultrasound, the mean fluorescence intensity was 2-fold higher than that with FITC-dextran alone. We also observed similar phenomena upon treatment with other sizes of FITC-dextran (MW 20,000 and 70,000) (Fig. 1(b), (c)). In addition, to assess the effect of molecular size on delivery efficiency, the fluorescence intensity was compared among FITC-dextrans (MW 4000, 20,000 and 70,000) delivered with BLs and ultrasound (Fig. 1(d)). The percentages of FITC-positive cells (M1 gated) were not affected by molecular weight, determined as 86.0% (MW: 4000), 87.3% (MW: 20,000), and 77.4% (MW: 70,000). On the other hand, the fluorescence intensity decreased as the molecular weight increased. The mean of fluorescence intensities were 24.5 (MW: 4000), 22.4 (MW: 20,000), and 16.5 (MW: 70,000).

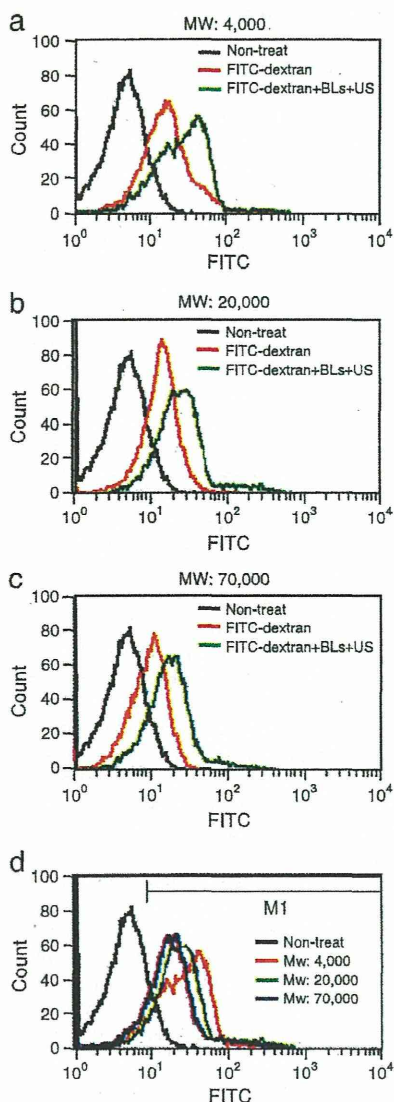

Fig. 1. Effect of molecular size on delivery into DCs using BLs and ultrasound. DCs were incubated with FITC-dextran, exposed to ultrasound in the presence of BLs, and washed with PBS. Delivery efficiency of FITC-dextran was analyzed using flow cytometry. Endocytosis by the DCs was inhibited by the inclusion of 10 mM sodium azide in all solutions and washes. Panels (a) to (c): Experiments were performed with FITC-dextran at a molecular weight of 4000, 20,000, or 70,000, respectively. Panel (d): Molecular weight dependency was analyzed following treatment with the combination of BLs and ultrasound. The percentages of M1 gated cell were quantified as follow: MW: 4000: 86.0%, MW: 20,000: 87.3%, MW: 70,000: 77.4%. The mean of fluorescent intensities were quantified as follow: MW: 4000: 24.5, MW: 20,000: 22.4, MW: 70,000: 16.5.

3.2. B16/BL6-extracted antigen delivery into DCs by BLs and ultrasound

Having demonstrated that the combination of BLs and ultrasound could deliver extracellular molecules of varying sizes, we sought to demonstrate that antigens extracted from B16/BL6 cells could be delivered into DCs by the same technique. Therefore, we assessed the delivery efficiency using Alexa Fluor 633-labeled antigens derived from B16/BL6 cells (Alexa-B16/BL6). As shown in Fig. 2, the DCs treated with antigens or the DCs treated with antigens and either BLs or ultrasound had fluorescence intensity profiles similar to those of untreated DCs. Flow cytometry confirmed this resemblance, with the percentages of Alexa-B16/BL6-positive cells (M2 gated) determined as 5.7% (antigen only), 6.5% (antigen and BLs), and 7.3% (antigen and ultrasound). In contrast, DCs treated with the combination of all three factors (antigens, BLs, and ultrasound) had an elevated fluorescence intensity profile compared with the other groups. Flow cytometry revealed that the percentage of Alexa-B16/BL6-positive cells was 74.1%.

3.3. Reduction in B16/BL6 lung metastasis following immunization with treated DCs

We employed an *in vivo* B16/BL6 experimental lung metastasis model to determine the anti-metastasis efficacy of DCs treated with tumor antigens delivered using BLs and ultrasound. C57BL/6 mice were immunized twice with bone marrow-derived DCs that were either untreated (no antigen exposure) or into which antigens had been delivered by one of four regimens (antigen alone; antigen + BLs; antigen + ultrasound; or antigen + BLs + ultrasound). As shown in Fig. 3(a), immunization with DCs that had been exposed to no antigen, antigen alone, or antigen with BLs *or* ultrasound weakly suppressed tumor metastasis. In contrast, immunization with DCs that had been exposed to antigens delivered via BLs *and* ultrasound reduced lung metastases four-fold, a decrease that was statistically significant ($P<0.05$) compared to the other groups. These numbers were consistent with the results of macroscopic inspection of lungs from the mice by stereoscopic microscopy, as shown in Fig. 3(b).

4. Discussion

The combination of ultrasound and microbubbles/nanobubbles has been reported to be an effective non-viral gene delivery method

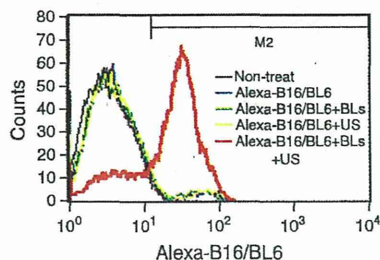

Fig. 2. Intracellular Alexa-B16/BL6 delivery into DCs using BLs and ultrasound. DCs were incubated with Alexa-labeled B16/BL6 extract, exposed (as indicated) to ultrasound and/or BLs, and washed with PBS. Delivery efficiency of Alexa-B16/BL6 was analyzed using flow cytometry. Endocytosis by the DCs was inhibited by the inclusion of 10 mM sodium azide in all solutions and washes. The percentages of M2 gated cell were quantified as follows: Alexa-B16/BL6: 5.7%; Alexa-B16/BL6 + BLs: 6.5%; Alexa-B16/BL6 + ultrasound 7.3%; Alexa-B16/BL6 + BLs + ultrasound: 74.1%.

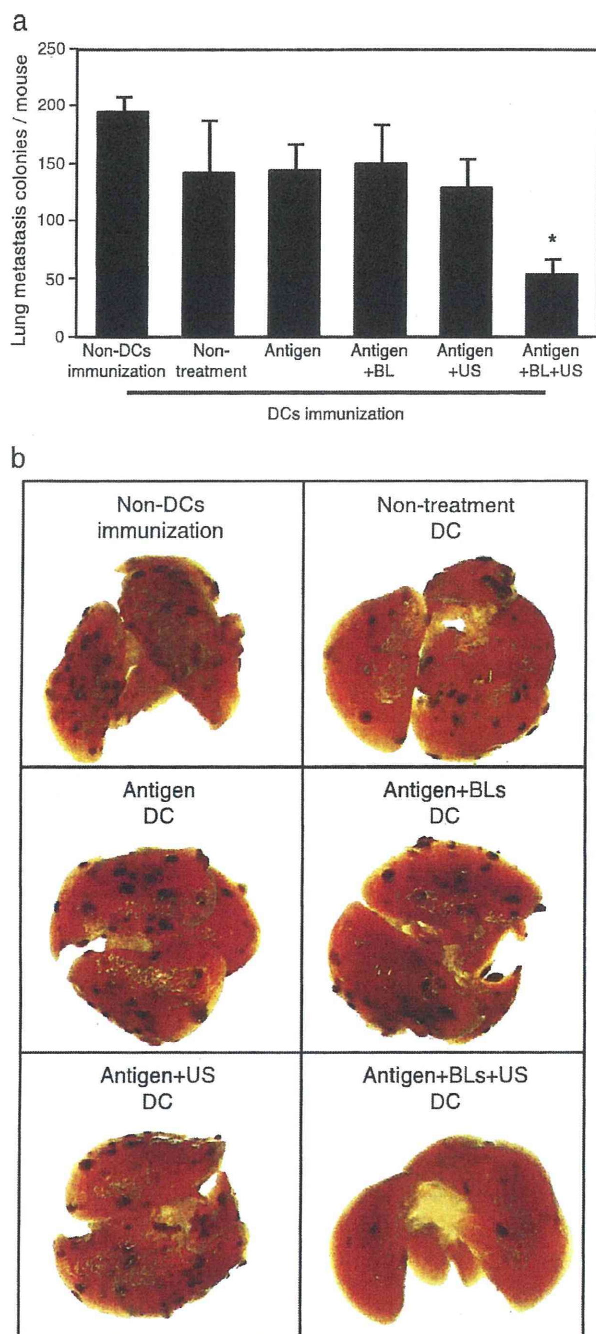

Fig. 3. Reduction of B16/BL6 lung metastasis following immunization with B16/BL6-treated DCs. DCs were treated with B16/BL6-extracted antigens and cultured as described in Materials and methods. C57BL/6 mice were immunized with the DCs twice with a one-week interval. One week after the second immunization, B16/BL6 cells were injected into the tail vein; after another two weeks, animals were sacrificed and lungs assessed for metastases. (a) Counts of lung metastatic colonies (means ± SDs; n = 6). *$P<0.05$ (ANOVA, comparing all DC-immunized groups). (b) Images of lung by stereomicroscope.

for whole cells. This technique also has been applied for peptide and protein delivery [38–40]. In a previous study, we proposed the use of this technique for the delivery of novel antigens into DCs for cancer immunotherapy [29]. Entry into cells is believed to reflect the presence of transient pores in the cell membrane, permitting extracellular molecules direct access to the cytosol [21,28,41]. The present study confirmed that antigen was delivered into DCs by the combination of BLs and ultrasound, with delivery observed despite inhibition of the endocytic pathway. Thus, BLs appear to play a role similar to that of microbubbles for ultrasound-mediated substrate delivery. The present study also demonstrated an inverse correlation between the size of the substrate (MW of FITC-dextran) and the efficiency of delivery (fluorescence intensity). These results are consistent with a dependence of antigen delivery on pore size, which in turn depends on the degree of sonoporated cell membranes by BLs. The effect of pore size is expected to limit the delivery of larger molecules. However, this effect should not prevent the application of BL/ultrasound methods for antigen delivery, given that we were able to demonstrate the immunotherapeutic potential of the technique in an *in vivo* mouse model of lung cancer metastasis. As shown in the present work, we still observed delivery (albeit at a reduced level) even for a molecule (FITC-dextran) with a MW of 70,000. FITC-dextran is a bulky polymer with a straight chain; by comparison, most proteins are tightly packed, with a resulting decrease in apparent size. Therefore, various antigens of a range of sizes should still be able to be delivered into DCs using the BL/ultrasound delivery system.

Melanoma is generally considered a highly immunogenic cancer, and several melanoma-associated antigens (e.g., MAGE, MART-1, gp-100) have been identified [8,42]. However, we thought that it was important to establish an antigen delivery system that was suitable for various extracts containing unknown TAAs, since such a technique would be applicable for the induction of a variety of CTL clones [6]. In the present study, we tested BL/ultrasound delivery with TAAs obtained (via butanol extraction) from B16/BL6 cells. The use of butanol extraction is especially appealing because this method has been shown to solubilize a subset of hydrophobic proteins [33] that would presumably include various known and novel TAAs. Antigens delivered to the cytosol of DCs are expected to induce MHC class I presentation by these DCs, in turn inducing antigen-specific CTLs [12]. In the present work, the utility of BL/ultrasound delivery of a crude extract was demonstrated for the B16/BL6 antigens both *in vitro* (Fig. 2) and *in vivo* (Fig. 3).

The *in vivo* assay described here tested the efficacy of B16/BL6 antigens in reducing lung metastasis. Specifically, DCs were exposed to antigens in the presence of BLs and ultrasound, and the treated cells were used for prophylactic immunization of mice. Immunization significantly decreased lung metastasis, indicating that the treated DCs induced a B16/BL6-specific anti-tumor immune response. Given the poor prognosis seen with metastases [3,4], and the challenge of preventing systemic metastasis in the long term, such a therapeutic strategy for metastatic cancer is desperately needed. From this perspective, DC-based cancer immunotherapy is an attractive option: this approach should induce systemic and specific immune responses via antigen presentation, and while also controlling metastasis and recurrence in the longer term via immunological memory [6]. Matheoud et al. reported that immunization of DCs has a potency to reduce the metastasis in therapeutic model (by post-immunization) [43]. To induce more effective immune responses, we are optimizing about antigen delivery for DCs by BLs/ultrasound. After optimization, we will attempt to prevent metastasis in therapeutic model. The combination of BLs and ultrasound is expected to induce effective immune response in DC-based cancer immunotherapy by delivering various TAAs into DCs for potential clinical applications.

Acknowledgments

The authors thank Mr. Eisuke Namai, Mr. Yasuyuki Shiono, Mr. Ken Osawa, Ms. Motoka Kawamura, Mr. Ryo Tanakadate, Mr. Kunihiko Matsuo, Mr. Yudai Kawashima, Mr. Hitoshi Uruga, and Ms. Mutsumi Seki (Teikyo University) for their technical assistance.